Article

# Influence of Inter- and Intramolecular Hydrogen Bonding on Kemp Decarboxylations from QM/MM Simulations

Orlando Acevedo, and William L. Jorgensen

*J. Am. Chem. Soc.*, **2005**, 127 (24), 8829-8834• DOI: 10.1021/ja051793y • Publication Date (Web): 26 May 2005



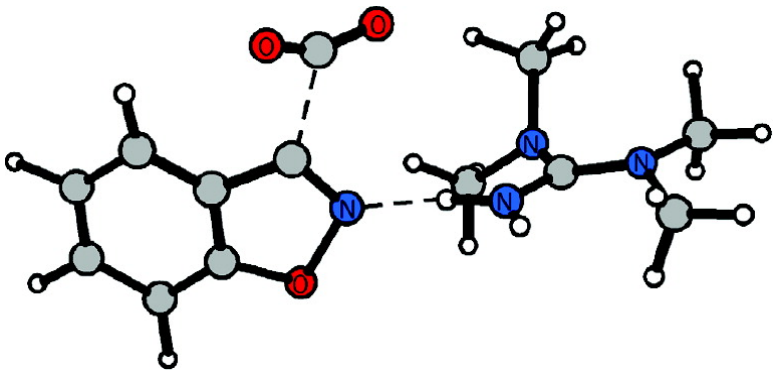

J|A|C|S
ARTICLES
Published on Web 05/26/2005

# Influence of Inter- and Intramolecular Hydrogen Bonding on Kemp Decarboxylations from QM/MM Simulations

Orlando Acevedo and William L. Jorgensen*

*Contribution from the Department of Chemistry, Yale University, 225 Prospect Street, New Haven, Connecticut 06520-8107*

Received March 21, 2005; E-mail: william.jorgensen@yale.edu

***Abstract:*** The Kemp decarboxylation reaction for benzisoxazole-3-carboxylic acid derivatives has been investigated using QM/MM calculations in protic and dipolar aprotic solvents. Aprotic solvents have been shown to accelerate the rates of reaction by 7−8 orders of magnitude over water; however, the inclusion of an internal hydrogen bond effectively inhibits the reaction with near solvent independence. The effects of solvation and intramolecular hydrogen bonding on the reactants, transition structures, and the rate of reaction are elucidated using two-dimensional potentials of mean force (PMF) derived from free energy perturbation calculations in Monte Carlo simulations (MC/FEP). Free energies of activation in six solvents have been computed to be in close agreement with experiment. Solute−solvent interaction energies show that poorer solvation of the reactant anion in the dipolar aprotic solvents is primarily responsible for the observed rate enhancements over protic media. In addition, a discrepancy for the experimental rate in chloroform has been studied in detail with the conclusion that ion-pairing between the reactant anion and tetramethylguanidinium counterion is responsible for the anomalously slow reaction rate. The overall quantitative success of the computations supports the present QM/MM/MC approach, which features PDDG/PM3 as the QM method.

## Introduction

The strong role of hydrogen bonding in the Kemp decarboxylation of 3-carboxybenzisoxazole (**1** in Scheme 1) is apparent in the dramatic rate acceleration of $10^8$ when the solvent is changed from protic to polar aprotic.[1,2] However, the addition of an intramolecular hydrogen bond (**3**) removes the rate enhancement by aprotic solvents, giving a uniformly slow rate with little solvent dependence.[2] To elucidate these dramatic kinetic effects at the atomic level, the present mixed quantum and molecular mechanics (QM/MM) simulations have been carried out. Specifically, the reactions of **1**−**3** have been investigated; free energies of activation have been computed and the effects of inter- and intramolecular hydrogen bonding for reactant and transition structures have been examined in water, methanol, chloroform, acetonitrile, THF, and DMSO. The transition structures have been located in solution with complete sampling of the geometry of the reacting systems and explicit representation of the solvent molecules. Special attention is paid to the anomalously slow reaction rate in chloroform. The importance of understanding medium effects on the Kemp eliminations is enhanced by the biological significance of related decarboxylations by, for example, pyruvate decarboxylase,[3] biotin enzymes,[4] decarboxylase antibodies,[5,6] and serum albumins.[6,7]

***Scheme 1.*** Kemp Decarboxylation for Derivatives of Benzisoxazole-3-carboxylic Acid

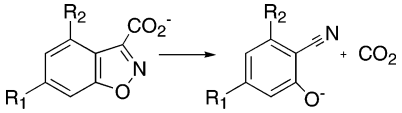


**1** ($R_1 = R_2 = H$)
**2** ($R_1 = OH$, $R_2 = H$)
**3** ($R_1 = H$, $R_2 = OH$)
**4** ($R_1 = NO_2$, $R_2 = H$)

## Computational Methods

QM/MM calculations,[8] as implemented in BOSS 4.6,[9] were carried out with the reacting system treated with the PDDG/PM3 method.[10] PDDG/PM3 has been extensively tested for gas-phase structures and energetics,[10] and it has given excellent results in solution-phase QM/MM studies of $S_N2$[11] and nucleophilic aromatic substitution reactions ($S_NAr$).[12] The solvent molecules are represented with the united-atom OPLS force field[13] for the nonaqueous solvents and with the TIP4P water model.[14] The systems consisted of the reactants, plus 395 solvent molecules for the nonaqueous solvents, or 740 molecules for water. To locate the minima and maxima on the free energy surface for the reaction, a two-dimensional free energy map was constructed in each case. Free energy perturbation (FEP) calculations were performed in conjunction with Metropolis Monte Carlo (MC) simulations at 25 °C and 1 atm. In this QM/MM implementation, the solute's intramolecular energy is treated quantum mechanically using PDDG/PM3; computation of the QM energy and atomic charges is performed for every solute move, occurring every 100 configurations. The partial charges were

(1) Kemp, D. S.; Paul, K. G. *J. Am. Chem. Soc.* **1975**, *97*, 7305−7312.
(2) Kemp, D. S.; Cox, D. D.; Paul, K. G. *J. Am. Chem. Soc.* **1975**, *97*, 7312−7318.
(3) (a) Recsei, P. A.; Snell, E. E. *Annu. Rev. Biochem.* **1984**, *53*, 357−387. (b) Marlier, J. F.; O'Leary, M. H. *J. Am. Chem. Soc.* **1986**, *108*, 4896−4899. (c) Lobell, M.; Crout, D. H. G. *J. Am. Chem. Soc.* **1996**, *118*, 1867−1873. (d) Sicinska, D.; Truhlar, D. G.; Paneth, P. *J. Am. Chem. Soc.* **2001**, *123*, 7683−7686.

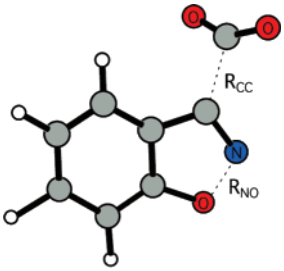


***Figure 1.*** Bond length variables, $R_{NO}$ and $R_{CC}$, for the Kemp decarboxylation of 3-carboxybenzisoxazole. Illustrated structure is the transition structure from gas-phase PDDG/PM3 calculations.

unscaled as obtained from the CM3 charge model[15] and the PDDG/PM3 wave function. Solute−solvent and solvent−solvent intermolecular cutoff distances of 12 Å were employed.

A new OPLS-AA five-site model for chloroform was developed with the usual reproduction of pure-liquid properties and free energies of solvation.[13,16] Standard bond-stretching and angle-bending parameters were assigned from the OPLS-AA parameter set.[17] The focus of the parametrization was on the development of the partial charges and nonbonded parameters. Initial atomic charges were computed using B3LYP/6-31G(d) calculations[18] and the CHELPG method[19] with the Gaussian 03 program.[20] Adjustments to the partial charges and the Lennard-Jones parameters were made so that the calculated properties for pure liquid chloroform agreed well with experiment.

## Results and Discussion

Changes in free energy were calculated by perturbing the distance between the nitrogen and oxygen of the isoxazole ($R_{NO}$) and the distance between the C3 and carboxylate carbon atoms ($R_{CC}$), as shown in Figure 1. The initial ranges for $R_{NO}$ and $R_{CC}$ were 1.35−2.35 Å with an increment of 0.05 Å. Each FEP calculation entailed 2.5 million (M) configurations of equilibration followed by 5 M configurations of averaging. As an example, the resultant map, which required 100 FEP calculations, for the reaction in methanol is shown in Figure 2. In all cases, transition structures and ground states were readily located. The number of single-point QM calculations that was performed to construct one such map was ca. 17 million. This emphasizes the need for use of semiempirical QM methods for such studies.

To locate the critical points more precisely, the regions surrounding the free energy minimum and maxima from the initial maps were explored using increments of 0.01 Å. This provided refined results for the reactions of **1**−**3** in several solvents, as summarized in Table 1. Measurements of kinetic isotope effects for the reaction indicate that, although aprotic solvents endow large rate enhancements, the transition-state structures do not show large variations.[21] Kemp and Paul also supported only subtle changes in the transition structure geometry in different solvents based on Hammett coefficient and entropy measurements.[1] The computed bond lengths in Table 1 confirm these expectations with modest changes for different solvents and reactants. In fact, there is little deviation from the PDDG/PM3 results for the parent reaction (**1**) in the gas phase with $R_{CC}$ and $R_{NO}$ distances of 2.11 and 1.74 Å. The transition structure occurs a little earlier in water owing to rapid decline in the hydrogen bonding to the carboxylate group as $R_{CC}$ increases.

The computed activation barriers for the reaction of 3-carboxybenzisoxazole (**1**) are summarized in Table 2. Uncertainties in the free energy barriers are calculated by propagating the standard deviation ($\sigma_i$) on each individual $\Delta G_i$. Smooth free energy profiles were obtained with statistical uncertainties ($1\sigma$) of only 0.01−0.03 kcal/mol in each window; thus, the overall uncertainties in the computed free energies of activation, $\Delta G^{\ddagger}$, are below 0.3 kcal/mol $(0.03^2 \times 120 \text{ windows})^{1/2}$. The computed $\Delta G^{\ddagger}$ values reproduce well the large rate enhancements in progressing from the protic to dipolar aprotic solvents. The quantitative accord is also good except for chloroform, which is discussed below.

Previous theoretical work on the Kemp decarboxylation has been carried out by Zipse et al.[22] They computed the changes in the free energy of solvation following a reaction path for benzisoxazole-3-carboxylate that was obtained from gas-phase ab initio calculations at the HF/6-31G(d) level.[22] The changes in free energy of solvation were computed using Monte Carlo simulations with the OPLS potential functions for the solvents and the BOSS program.[9,23] In this approach the reaction path was fixed and no QM calculations were performed during the MC simulations. Table 3 lists their reported solvent effects for the reaction with and without two explicit water molecules in addition to the PDDG/PM3 values computed in the present study for five different solvents. The present QM/MM simulations using the PDDG/PM3 method show improved agreement with the experimental data.

The reaction of **1** was also investigated by Gao using gas- and aqueous-phase calculations.[24,25] The gas-phase reaction path was determined at the HF/3-21G level, predicting a $\Delta H^{\ddagger}$ value

(4) (a) Rahil, J.; You, S.; Kluger, R. *J. Am. Chem. Soc.* **1996**, *118*, 12495−12498. (b) Gao, D.; Pan, Y. K. *J. Org. Chem.* **1999**, *64*, 4492−4501.
(5) (a) Lewis, C.; Kreamer, T.; Robinson, S.; Hilvert, D. *Science* **1991**, *253*, 1019−1022. (b) Hotta, K.; Lange, H.; Tantillo, D. J.; Houk, K. N.; Hilvert, D.; Wilson, I. A. *J. Mol. Biol.* **2000**, *302*, 1213−1225. (c) Hotta, K.; Wilson, I. A.; Hilvert, D. *Biochemistry* **2002**, *41*, 772−779.
(6) Hu, Y.; Houk, K. N.; Kikuchi, K.; Hotta, K.; Hilvert, D. *J. Am. Chem. Soc.* **2004**, *126*, 8197−8205.
(7) (a) Hollfelder, F.; Kirby, A. J.; Tawfik, D. S. *Nature* **1996**, *383*, 60−63. (b) Kikuchi, K.; Thorn, S. N.; Hilvert, D. *J. Am. Chem. Soc.* **1996**, *118*, 8184−8185. (c) Hollfelder, F.; Kirby, A. J.; Tawfik, D. S.; Kikuchi, K.; Hilvert, D. *J. Am. Chem. Soc.* **2000**, *122*, 1022−1029.
(8) (a) Warshel, A.; Levitt, M. *J. Mol. Biol.* **1976**, *103*, 227−249. (b) Kaminski, G. A.; Jorgensen, W. L. *J. Phys. Chem. B* **1998**, *102*, 1787−1796.
(9) Jorgensen, W. L. *BOSS*, Version 4.6; Yale University: New Haven, CT, 2004.
(10) (a) Repasky, M. P.; Chandrasekhar, J.; Jorgensen, W. L. *J. Comput. Chem.* **2002**, *23*, 1601−1622. (b) Tubert-Brohman, I.; Guimarães, C. R. W.; Repasky, M. P.; Jorgensen, W. L. *J. Comput. Chem.* **2003**, *25*, 138−150.
(11) Vayner, G.; Houk, K. N.; Jorgensen, W. L.; Brauman, J. I. *J. Am. Chem. Soc.* **2004**, *126*, 9054−9058.
(12) Acevedo, O.; Jorgensen, W. L. *Org. Lett.* **2004**, *6*, 2881−2884.
(13) (a) Jorgensen, W. L.; Briggs, J. M.; Contreras, M. L. *J. Phys. Chem.* **1990**, *94*, 1683−1686. (b) Briggs, J. M.; Matsui, T.; Jorgensen, W. L. *J. Comput. Chem.* **1990**, *11*, 958−971. (c) Jorgensen, W. L.; Briggs, J. M. *Mol. Phys.* **1988**, *63*, 547−558.
(14) Jorgensen, W. L.; Chandrasekhar, J.; Madura, J. D.; Impey, W.; Klein, M. L. *J. Chem. Phys.* **1983**, *79*, 926−935.
(15) Thompson, J. D.; Cramer, C. J.; Truhlar, D. G. *J. Comput. Chem.* **2003**, *24*, 1291−1304.
(16) Rizzo, R.; Jorgensen, W. L. *J. Am. Chem. Soc.* **1999**, *121*, 4827−4836.
(17) Jorgensen, W. L.; Maxwell, D. S.; Tirado-Rives, J. *J. Am. Chem. Soc.* **1996**, *118*, 11225−11236.
(18) (a) Becke, A. D. *J. Chem. Phys.* **1993**, *98*, 5648−5652. (b) Lee, C.; Yang, W.; Parr, R. G. *Phys. Rev.* **1988**, *37*, 785−789.
(19) Breneman, C. M.; Wiberg, K. B. *J. Comput. Chem.* **1990**, *11*, 361−373.
(20) Frisch, M. J. *Gaussian 03*, Revision A.1; Gaussian, Inc.: Pittsburgh, PA, 2003 (full reference given in the Supporting Information).
(21) (a) Czyryca, P.; Paneth, P. *J. Org. Chem.* **1997**, *62*, 7305−7309. (b) Lewis, C.; Paneth, P.; O'Leary, M. H.; Hilvert, D. *J. Am. Chem. Soc.* **1993**, *115*, 1410−1413.
(22) Zipse, H.; Apaydin, G.; Houk, K. N. *J. Am. Chem. Soc.* **1995**, *117*, 8608−8617.
(23) Jorgensen, W. L. *J. Phys. Chem.* **1986**, *90*, 1276−1284.
(24) Gao, J. *J. Am. Chem. Soc.* **1995**, *117*, 8600−8607.
(25) Gao, J. *Acc. Chem. Res.* **1996**, *29*, 298−305.

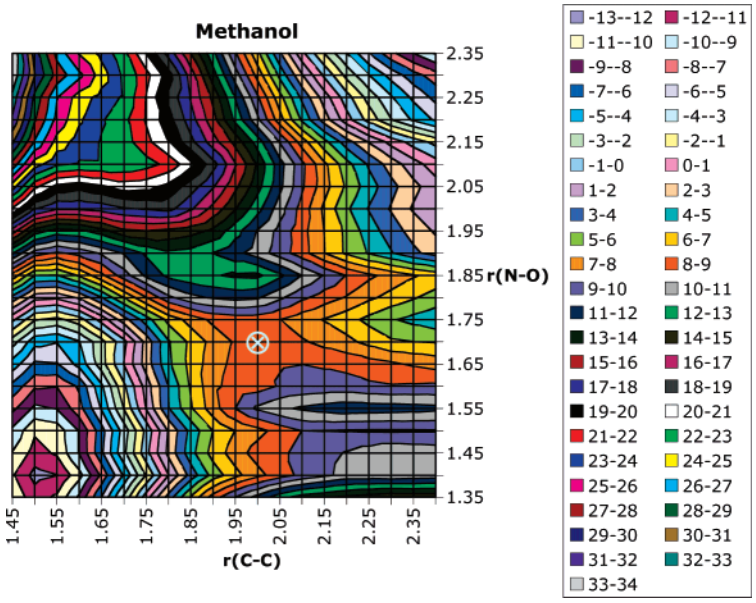


***Figure 2.*** Two-dimensional potential of mean force for the reaction of **1** in methanol used to identify the free energy maxima and minima. ⊗ Indicates the location of the transition structure. All distances in Å and relative free energies in kcal/mol.

***Table 1.*** Computed Bond Lengths (Å) for 3-Carboxybenzisoxazole Transition Structures at 25 °C and 1 atm

| **1** ($R_1$ = H, $R_2$ = H) | water | $CH_3OH$ | $CHCl_3$ | $CH_3CN$ | THF |
|---|---|---|---|---|---|
| $R_{CC}$ | 2.00 | 2.02 | 2.07 | 2.02 | 2.05 |
| $R_{NO}$ | 1.75 | 1.70 | 1.71 | 1.75 | 1.74 |
| **2** ($R_1$ = OH, $R_2$ = H) | water | $CH_3CN$ | DMSO | | |
| $R_{CC}$ | 1.98 | 2.06 | 2.16 | | |
| $R_{NO}$ | 1.75 | 1.69 | 1.67 | | |
| **3** ($R_1$ = H, $R_2$ = OH) | water | $CH_3CN$ | DMSO | | |
| $R_{CC}$ | 1.97 | 2.04 | 2.06 | | |
| $R_{NO}$ | 1.71 | 1.74 | 1.75 | | |

***Table 2.*** Free Energy of Activation, $\Delta G^{\ddagger}$ (kcal/mol), for the Kemp Decarboxylation of **1** from QM/MM/MC Simulations

| | calc[a] | exptl[b] |
|---|---|---|
| water | 24.9 | 26.4 (± 1.5) |
| methanol | 22.5 | 24.7 |
| chloroform | 14.8 | 24.0 |
| acetonitrile | 15.5 | 19.4 |
| THF | 12.1 | 19.1 |

[a] Statistical uncertainties ($1\sigma$) are less than 0.3 kcal/mol. [b] Free energies of activation from ref 1.

***Table 3.*** Comparison of Relative Free Energies of Activation, $\Delta\Delta G^{\ddagger}$ (kcal/mol), for the Kemp Decarboxylation of **1** in Solution Using the QM/MM/MC Method

| | water | MeOH | $CHCl_3$ | $CH_3CN$ | THF |
|---|---|---|---|---|---|
| PDDG/PM3 | 0 | −2.43 | −10.1 | −9.44 | −12.8 |
| HF/6-31G(d)[a] | 0 | −5.22 | −14.7 | −11.2 | −16.9 |
| HF/6-31G(d) + $2H_2O$[a] | 0 | −4.58 | −13.8 | −13.1 | −16.1 |
| exptl[b] | 0 | −1.67 | −2.41 | −7.01 | −7.31 |

[a] Reference 22. [b] Reference 1. Values extrapolated from correlation of benzisoxazole and 6-nitrobenzisoxazole-3-carboxylate rate data.

of 17.4 kcal/mol at 298 K.[24] PDDG/PM3 gives a $\Delta H^{\ddagger}$ of 11.1 kcal/mol in a vacuum, while MP2/6-31G(d)//HF/6-31G(d) with zero-point energy corrections yields a gas-phase barrier of 19.1 kcal/mol.[22] Gao also investigated benzisoxazole-3-carboxylate in aqueous solution using MC simulations with a hybrid AM1/TIP3P potential; the computed QM/MM/MC activation free energy of 26.1 ± 0.3 kcal/mol[24] in water agrees well with experiment and our computed results (Table 2). Electron density analysis on gas-phase and aqueous wave functions revealed that, for the ground state, charge polarization is greatest for the carboxylate group, whereas for the transition state it shifts to the isoxazole oxygen and nitrogen.[24,25]

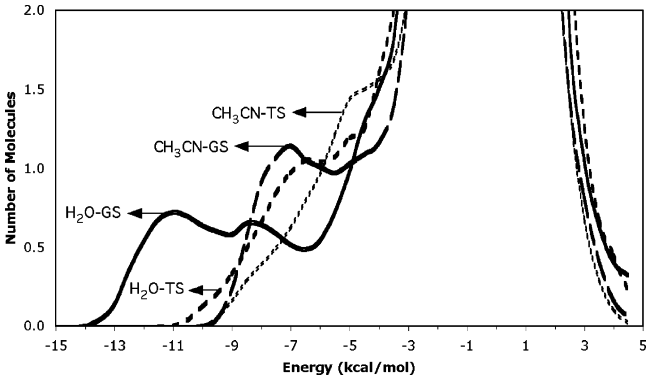


***Figure 3.*** Solute−solvent energy pair distributions for the reaction of **1** ($R_1$ = H, $R_2$ = H) in water and acetonitrile for the reactant (GS) and transition structure (TS). The ordinate records the number of solvent molecules that interact with the solutes with their interaction energy on the abscissa. Units for the ordinate are number of molecules per kcal/mol.

Detailed insights on the changes in solvation along the reaction paths are also available from the present QM/MM/MC calculations. In particular, the solute−solvent energy pair distributions record the average number of solvent molecules that interact with the solute and the associated energy. The results for the Kemp decarboxylation in water and acetonitrile are shown in Figure 3; the results for the other solvents can be found in the Supporting Information. Hydrogen bonding in protic solvents and the most favorable interaction energies in aprotic solvents are reflected in the left-most region, with energies more attractive than ca. −5 kcal/mol. The large bands near 0 kcal/mol result from the many distant solvent molecules in outer shells.

***Table 4.*** OPLS-AA Nonbonded Parameters for All-Atom Chloroform

| site | $q$, e | $\sigma$, Å | $\epsilon$, kcal/mol |
|---|---|---|---|
| C | −0.076 | 4.10 | 0.05 |
| Cl | −0.029 | 3.40 | 0.30 |
| H | 0.163 | 2.42 | 0.03 |

***Table 5.*** OPLS-AA Stretching and Bending Parameters for All-Atom Chloroform

| bond | $k_r$ (kcal mol$^{-1}$ Å$^{-2}$) | $r_0$ (Å) |
|---|---|---|
| C−H | 437.0 | 1.086 |
| C−Cl | 300.0 | 1.766 |
| **angle** | $k_\theta$ (kcal mol$^{-1}$ rad$^{-2}$) | $\theta_0$ (deg) |
| H−C−Cl | 60.0 | 107.7 |
| Cl−C−Cl | 78.0 | 111.4 |

The outstanding features in Figure 3 are the low-energy bands for the reactants compared to the transition state in the protic solvent, arising from the water molecules forming stronger hydrogen bonds with the carboxylate anion. The band for the aprotic solvent reflects less favorable ion−dipole interactions occurring for the reactant. Integration of the bands from −15 to −6 kcal/mol yields 8 or 9 water molecules, while the band from −11 to −5.5 kcal/mol for acetonitrile contains 7 solvent molecules. Clearly, a major source of the rate enhancement in the aprotic solvents comes from reduced stabilization of the reactant compared to that provided by the hydrogen bonding in water. Solvation of the charge-delocalized transition structures appears comparatively similar for both water and acetonitrile, as indicated by the bands centered around −7 and −5 kcal/mol, respectively. Although the interactions remain more favorable for water than acetonitrile, the difference is small compared to that for the reactants. Thus, as expected,[1,2] poorer solvation of the reactant anion in dipolar aprotic solvents is the principal contributor to the enhanced reaction rates in comparison with protic solvents.

**Origin of the Slow Rate in Chloroform.** An interesting point with the Kemp reaction is that it seems anomalously slow in chloroform. For **4** ($R_1 = NO_2$, $R_2 = H$), the observed relative rates at 30 °C are 1 (water), 34 (methanol), 100 ($CHCl_3$), 6350 ($CH_2Cl_2$), $0.54 \times 10^5$ (THF), $3.9 \times 10^5$ ($CH_3CN$), and $1.4 \times 10^6$ (DMSO).[1] The counterion is 1,1,3,3-tetramethylguanidinium (TMG), and the chloroform was dried by distillation over phosphorus pentoxide. The suggestion was made that chloroform may be acting as a hydrogen bond donor.[1] This notion arises occasionally, though chloroform's properties designate it as an apolar aprotic solvent; $CH_2Cl_2$ is more polar. The results in Table 1 for the reaction of **1** using PDDG/PM3 and the four-site (no H) OPLS-UA model of chloroform predict a large rate increase similar to that for $CH_3CN$. To address this issue, a new five-site OPLS-AA model for chloroform was created (Tables 4 and 5) in a fashion similar to previous work.[16] Explicit inclusion of the hydrogen in chloroform might facilitate hydrogen bonding.

MC simulations were run for this model with all molecules fully flexible in the gas and pure liquid phases. For the latter, 395 chloroform molecules were used in simulations covering 5 M configurations of equilibration and 10 M configurations of averaging. The computed values for the liquid density and heat of vaporization are in excellent agreement with experiment (Table 6). It should be noted that the all-atom chloroform model yields a gas-phase dipole moment of 1.08 D, which is slightly enhanced over the experimental value of 1.01 D.[26]

***Table 6.*** Density (g/cm$^3$) and Heat of Vaporization (kcal/mol) for All-Atom Chloroform at 25 °C and 1 atm

| | $\rho$(calc) | $\rho$(exptl)[a] | $\Delta H_v$(calc) | $\Delta H_v$(exptl)[b] |
|---|---|---|---|---|
| $CHCl_3$-AA | 1.49 | 1.473 | 7.41 | 7.43 |

[a] Reference 27. [b] Reference 28.

The all-atom chloroform model was then used in analogous QM/MM calculations for the reaction of **1**. However, this did not solve the dilemma, as the resultant free energy of activation (14.2 kcal/mol) was nearly identical to the result with the united-atom model (14.8 kcal/mol). Another possibility is that the chloroform was not completely dry in the experiments, although much care appears to have been taken in this regard.[1] Some initial QM/MM investigations were performed for the reaction of **1** with the united-atom chloroform model including the addition of a water molecule; however, the increase in the free energy of activation was modest, ca. 1 kcal/mol.

Thus, we turned our attention to possible ion-pairing. That is, the unusually slow rate in chloroform could be due to preferential stabilization of the reactant by the TMG counterion. Previously, theoretical calculations were performed by Zipse et al., complexing TMG to the carboxylate group in **1** and optimizing the ground- and transition-state structures using HF/6-31G(d).[22] The computed gas-phase activation barrier was extremely large (62.4 kcal/mol) at the MP2/6-31G(d)//HF/6-31G(d) level. Further MC studies did show an increase in the $\Delta\Delta G^{\ddagger}$ between acetonitrile and THF from −3.8 to −1.5 kcal/mol without and with TMG, respectively, while the experimental difference is −0.3 kcal/mol.[1] On the experimental side, Kemp and Paul observed that use of the strong base, TMG, or the weaker base, triethylamine, has little to no influence on the rates of reaction in nearly all dipolar aprotic solvents.[1] However, for the reaction in aprotic solvents of low polarity, such as chloroform, the observed rate constants are not cation independent.[1] Thus, the QM/MM simulations were repeated for the reaction of **1** in united-atom chloroform with the addition of a TMG ion initially placed near the carboxylate group of the reactant (Figure 4). Both ions were treated quantum mechanically (PDDG/PM3) as separate solutes in the QM/MM simulation in a box of 395 chloroform molecules. The ions were fully flexible, and the MC simulation for each FEP window again consisted of 2.5 M configurations of equilibration and 5 M configurations of averaging. The TMG wanders during the reaction from the vicinity of the carboxylate group in the reactant toward the isoxazole in the transition state, following the redistribution of negative charge. Excellent agreement with experiment is now obtained for the activation free energy (Table 7); inclusion of the counterion does account for the slow rate observed in chloroform.

Ion-pairing with the TMG ion is expected to decrease with increasing solvent polarity and may also be responsible for the residual differences between the computed and observed values in acetonitrile and THF (Table 3).

**Influence of Intramolecular Hydrogen Bonding.** For the Kemp decarboxylation of **1** in protic solvents, hydrogen bonding

(26) In *CRC Handbook of Chemsitry and Physics*; Weast, R. C., Ed.; CRC Press: Boca Raton, FL, 1988; pp E52−54.

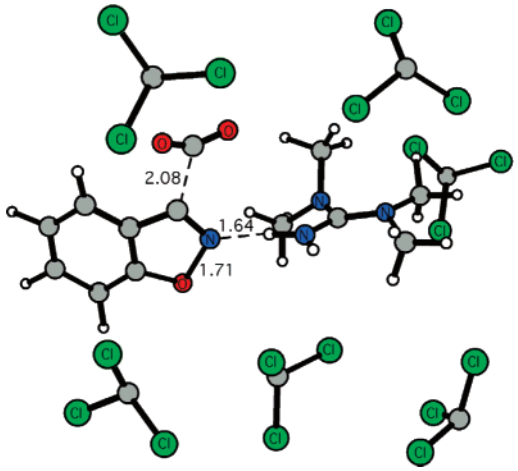


***Figure 4.*** Snapshot of a transition structure for the reaction of **1** with a TMG counterion in united-atom chloroform (nearby solvent molecules are illustrated) from the QM/MM/MC simulation. Distances in Å.

***Table 7.*** Influence of the Addition of a Tetramethylguanidinium Ion on the Computed $\Delta G^{\ddagger}$ (kcal/mol) for the Decarboxylation of **1**

| | $CHCl_3$-UA | $CHCl_3$-UA + TMG | exptl[a] |
|---|---|---|---|
| $\Delta G^{\ddagger}$ | 14.8 | 27.7 | 24.0 |

[a] Reference 1.

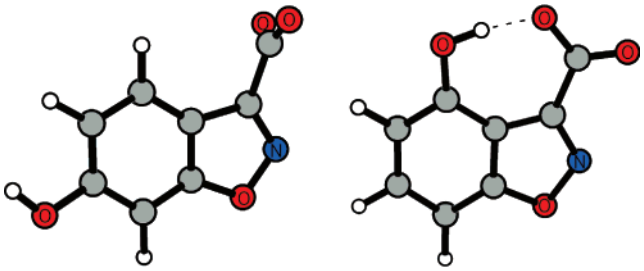

***Figure 5.*** PDDG/PM3 optimized gas-phase geometries for **2** and **3**.

***Table 8.*** Free Energies of Activation, $\Delta G^{\ddagger}$ (kcal/mol), for the Kemp Decarboxylation of **2** and **3** from QM/MM/MC Simulations

| | **2** | exptl[a] | **3** | exptl[a] |
|---|---|---|---|---|
| water | 25.8 | 25.8[b] | 25.2 | 25.6 |
| DMSO | 15.9 | 15.9 | 23.4 | 23.6 |
| acetonitrile | 15.6 | 19.4[c] | 22.4 | 26.3 |

[a] Reference 2. [b] $R_1 = OCH_3$, $R_2 = H$, ref 1. [c] $R_1 = H$, $R_2 = H$.

to the reactant is the major factor inhibiting reactivity. If the rate acceleration in dipolar aprotic solvents is a result of the lessened stabilization of the reactant anion, then a reactant with an intramolecular hydrogen bond to the carboxylate is expected to be less reactive in all solvents. Indeed, Kemp and co-workers observed that the internally hydrogen-bonded 4-hydroxy-3-carboxybenzisoxazoles such as **3** exhibit essentially identical reaction rates in water, acetonitrile, and DMSO, negating the catalytic effects of aprotic solvents.[2] This effect was also explored with QM/MM simulations for **3** and the isomeric 6-hydroxy-3-carboxybenzisoxazole, **2**, in water, DMSO, and acetonitrile (Figure 5). The resultant free energies of activations are reported in Table 8.

The QM/MM findings agree exceedingly well with the experimentally observed free energies of activation; the results are essentially identical in water and DMSO in view of the uncertainties in the computations, ±0.3 kcal/mol. An estimate

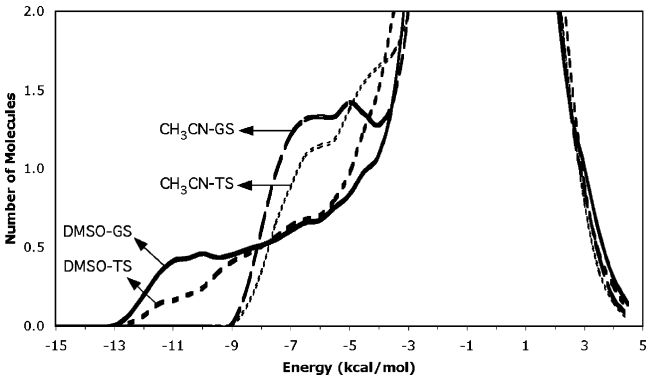


***Figure 6.*** Solute−solvent energy pair distributions for the reaction of **3** in DMSO and acetonitrile for the reactant (GS) and transition structure (TS). Details are as in Figure 3.

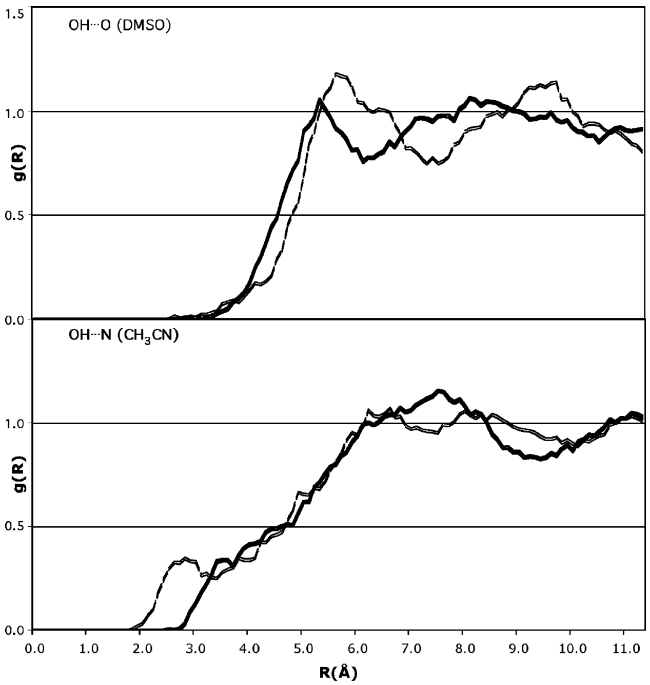


***Figure 7.*** Computed OH−O (DMSO) and OH−N ($CH_3CN$) radial distribution functions for the reactant (solid curve) and transition state (dashed curve) for the reaction of **3**.

of strength of the intramolecular hydrogen bond in **3** can be obtained from the difference in the free energies of activation for **2** and **3**; in DMSO, the computed and experimental values are 7.5 and 7.7 kcal/mol, while they are 6.8 and 6.9 kcal/mol in acetonitrile. The ability of the PDDG/PM3-based QM/MM calculations to represent well the internal hydrogen bonding is notable. In analogous work using AM1, the strength of the internal hydrogen bond was slight and large rate accelerations were erroneously predicted for **3** in DMSO and acetonitrile over water.[29]

As a further point of interest, a 95-fold rate increase for the intramolecularly hydrogen bonded **3** is observed experimentally when the solvent is changed from acetonitrile to DMSO, whereas the rates for derivatives of the carboxybenzisoxazoles in this pair of solvents typically differ by no more than a factor

(27) Sanni, S. A.; Hutchison, P. *J. Chem. Eng. Data* **1973**, *18*, 317−322.
(28) Majer, V.; Svab, L.; Svoboda, V. *J. Chem. Thermodyn.* **1980**, *12*, 843−847.
(29) Ostrovsky, D. Ph.D. Thesis, Yale University, New Haven, CT, 2003.

of 10.[2] It was suggested that strong hydrogen-bond accepting ability for DMSO competes with the 3-carboxylate for hydrogen bonding with the hydroxyl group.[2] Solute−solvent energy pair distributions have been computed, and DMSO is found to provide more favorable interactions overall for **3** when compared to acetonitrile (Figure 6; see Supporting Information for additional solute−solvent energy pair distribution plots for **2** and **3**). The specific interactions between the hydroxyl group of **3** and the solvent molecules were further pursued via radial distribution functions for the reactant and transition structures. Hydrogen bonds between the hydroxyl H of **3** and the oxygen of DMSO or nitrogen of acetonitrile would be reflected in contacts shorter than 2.5 Å. As evidenced in Figure 7, neither solvent is hydrogen bonding with the OH group of reactant **3**; the more favorable interactions found in DMSO over acetonitrile (Figure 6) are a result of stronger ion−dipole interactions. However, hydrogen bonding is indicated for the OH group in the transition structure for the reaction of **3** in acetonitrile, though still not in DMSO. Thus, the present results do not support a competition between DMSO and the carboxylate group for hydrogen bonding in **3**.

## Conclusion

QM/MM/MC simulations have been applied to Kemp decarboxylation reactions with good success in reproducing the observed substrate and solvent effects on the free energy of activation. The geometries of the transition states were found to be similar for all cases in both dipolar aprotic and protic solvents, consistent with experimental results. The overall quantitative success supports the utility of the present QM/MM/MC approach using PDDG/PM3 as the QM method. Hydrogen bonding was determined to be the most important factor reducing the rates of reaction through preferential stabilization of the reactant anion via intermolecular interactions in protic solvents or intramolecular hydrogen bonding in **3**. Hydrogen bonding is more favorable for the reactant anions than for the more charge-delocalized transition structures. In apolar aprotic solvents, such as chloroform, ion-pairing with a TMG counterion has also been demonstrated to retard the rate of reaction by analogous interactions favoring the charge-localized reactant.

**Acknowledgment.** Gratitude is expressed to the National Science Foundation (CHE-0130996) and the National Institutes of Health (GM032136) for support of this research.

**Supporting Information Available:** Additional energy pair distributions for the Kemp reactions are provided. This material is available free of charge via the Internet at http://pubs.acs.org.

JA051793Y